Inorg. Chem. **2008**, *47*, 3509−3514

Binding of Catechols to Mononuclear Titanium(IV) and to 1- and 5-nm TiO_2 Nanoparticles

Carol Creutz* and Mei H. Chou

Chemistry Department, Brookhaven National Laboratory, Upton, New York 11973-5000

Received August 27, 2007

The binding of catechol derivatives (LH_2 = catechol, 4-methyl catechol, 4-t-butyl catechol, and dopamine) to 1- and 4.7-nm TiO_2 nanoparticles in aqueous, pH 3.5 suspensions has been characterized by UV−vis spectroscopy. The binding constants derived from Benesi−Hildebrand plots are (2−4) × 10^3 M^{-1} for the 1-nm nanoparticles and (0.4–1) × 10^4 M^{-1} for the 4.7-nm particles. $Ti^{IV}L_3$ complexes were prepared from the same catechols. The L = methyl catechol, and dopamine complexes are reported for the first time. The TiL_3 reduction potentials are not very sensitive to the nature of the catechol nor evidently are the binding constants to TiO_2 nanoparticles. The intense ($\varepsilon \geq 10^3$ M^{-1} cm^{-1}), about 400-nm, ligand-to-metal charge-transfer (LMCT) absorptions of the nanoparticle complexes are compared with those of the TiL_3 complexes (ε 10^4 M^{-1} cm^{-1}) which lie in the same spectral region. The nanoparticle colors are attributed (as are the colors of the $Ti^{IV}L_3$ complexes) to the tails of the about 400-nm LMCT bands.

Introduction

Water-soluble complexes of Ti(IV) are of interest in environmental,[1] biological,[2] and materials chemistry,[3] and catechol (1,2-dihydroxybenzene) type ligands are of interest in their own right.[4,5] Moser and Grätzel were the first to report the orange color produced upon adsorption of catechol on TiO_2.[6] As noted by Lian,[7] the absorption responsible for the color is similar to the ligand-to-metal charge-transfer (LMCT) absorption observed for mononuclear titanium(IV) complexes.[8] Such binding has been observed for nanoparticles and nanocrystals[9] and has received some attention in recent years.[6,7,10–15] Electronic structure calculations of the catechol−nanoparticle complexes are consistent with the LMCT description of the transition.[16,17] Several studies have implicated two types of binding to the TiO_2 surface for catechol or its derivatives.[10,13] In a very recent Raman study, chelate formation was proposed to involve single, four-coordinate Ti sites, and lower affinity "molecular adsorption" was proposed to involve adjacent Ti and O sites.[18] The LMCT absorption is attributed to the chelated species.[18] Rajh et al. have invoked special binding sites on small (<2 nm) nanoparticles that are said to be produced by the nanoparticle surface curvature. For the extremely well-studied P-25 (30-nm particles), the binding sites are associated with singly coordinated, acidic Ti sites.[19]

* To whom correspondence should be addressed. E-mail: ccreutz@bnl.gov.

(1) Vasudevan, D.; Stone, A. T. *Environ. Sci. Technol.* **1996**, *30*, 1604–1613.
(2) Endres, P. J.; Paunesku, T.; Vogt, S.; Meade, T. J.; Woloschak, G. E. *J. Am. Chem. Soc.* **2007**, *129*, 15760–15761.
(3) Uppal, R.; Incarvito, C. D.; Lakshmi, K. V.; Valentine, A. M. *Inorg. Chem.* **2006**, *45*, 1795–1804.
(4) Zanello, P.; Corsini, M. *Coord. Chem. Rev.* **2006**, *250*, 2000–2022.
(5) Sever, M. J.; Wilker, J. J. *Dalton Trans.* **2004**, 1061–1072.
(6) Moser, J.; Punchihewa, S.; Infelta, P. P.; Grätzel, M. *Langmuir* **1991**, *7*, 3012–3018.
(7) Wang, Y.; Hang, K.; Anderson, N. A.; Lian, T. *J. Phys. Chem. B.* **2003**, *107*, 9434–9440.
(8) Borgias, B. A.; Cooper, S. R.; Koh, Y. B.; Raymond, K. N. *Inorg. Chem.* **1984**, *23*, 1009–1016.
(9) Hao, E. C.; Anderson, N. A.; Asbury, J. B.; Lian, T. Q. *J. Phys. Chem. B* **2002**, *106*, 10191–10198.
(10) Rodriguez, R.; Blesa, M. A.; Regazzoni, A. E. *J. Colloid Interface Sci.* **1996**, *177*, 122–131.
(11) Liu, Y. M.; Dadap, J. I.; Zimdars, D.; Eisenthal, K. B. *J. Phys. Chem B* **1999**, *103*, 2480–2486.
(12) Weng, Y.-X.; Wang, Y.-Q.; Asbury, J. B.; Ghosh, H. N.; Lian, T. *J.Phys. Chem. B* **2000**, *104*, 93–104.
(13) Rajh, T.; Chen, L. X.; Lukas, K.; Liu, T.; Thurnauer, M. C.; Tiede, D. M. *J. Phys. Chem. B* **2002**, *106*, 10543–10552.
(14) Rajh, T.; Nedeljkovic, J. M.; Chen, L. X.; Poluektov, O.; Thurnauer, M. C. *J. Phys. Chem. B.* **1999**, *103*, 3515–3519.
(15) Rajh, T.; Saponjic, Z.; Liu, J.; Dimitrijevic, N. M.; Scherer, N. F.; Vega-Arroyo, M.; Zapol, P.; Curtiss, L. A.; Thurnauer, M. C. *Nano Lett.* **2004**, *4*, 1017–1023.
(16) Redfern, P. C.; Zapol, P.; Curtiss, L. A.; Rajh, T.; Thurnauer, M. C. *J. Phys. Chem B* **2003**, *107*, 11419–11427.
(17) Rego, L. G. C.; Batista, V. S. *J. Am. Chem. Soc.* **2003**, *125*, 7989–7997.
(18) Lana-Villarreal, T.; Rodes, A.; Pérez, J. M.; Gómez, R. *J. Am. Chem. Soc.* **2005**, *127*, 12601–12611.
(19) Bourikas, K.; Stylidi, M.; Kondarides, D. I.; Verykios, X. E. *Langmuir* **2005**, *21*, 9222–9230.

10.1021/ic701687k CCC: $40.75
Published on Web 03/27/2008

Chart 1. Abbreviations and Structures of the Catechols Used

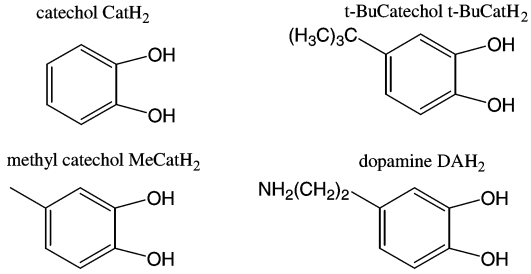

Although nanoparticulate TiO_2 has been the subject of intense study because of its applications to a range of photochemical applications, the nature of the electron-acceptor states remains poorly understood.[20] Electron photoinjection from an adsorbate may proceed directly into the delocalized conduction band or to a more localized site. The nature of the process(es) has been probed via transient absorption studies,[7,21] time-resolved 2-photon photoemission,[22] and by electroabsorption experiments.[23] Thus, Harris et al. recently reported electroabsorption results for TiO_2-bound metal cyano complexes that implicate a localized acceptor state at about 0.5 eV above the bottom of the conduction band.[24] In principle, the two injection modes may be distinguished spectroscopically because the absorption profiles are predicted to differ for the two possibilities.[24,25] As will be seen, consistent with several theoretical studies, comparison of the electronic spectroscopy of the nanoparticulate and mononuclear Ti(IV) complexes is consistent with these "metal-to-particle transitions" being due to localized, LMCT transitions.

Here we consider small TiO_2 particles that have two to three times the surface area of P-25. It is of interest to compare the binding for the various particles and to try to determine to what extent the binding sites differ among the different materials. Wang et al. compared the transient dynamics of mononuclear TiL_3^{2-} and TiO_2-adsorbed catechol.[7] The purpose of the experiments described here was to characterize the binding of catechol and derivatives to small TiO_2 nanoparticles, to determine their electronic absorption spectra, and to compare them with the electronic absorption spectra of the corresponding mononuclear Ti(IV) tris complexes. The shape of the absorption profile and its behavior at long wavelength are compared with those of the simple coordination complexes, for which there can be no delocalized electron-acceptor state. Abbreviations and structures of the catechols studied are presented in Chart 1.

Experimental Section

Preparation and Characterization of Titanium Catechol Complexes. The literature method reported for preparation of the catechol complex[8] was utilized. The mononuclear TiL_3 complexes resulted with L = MeCat and DA;

$$Ti(OH)_2^{2+} + 3Cat^{2-} + 4H^+ \rightarrow [Ti(Cat)_3]^{2-} + 6H_2O \qquad (1)$$

however, with L = t-BuCat, the previously described, bridged species $(NH_4)_2[Ti(tBuCat)_2(HtBuCat)]_2$ resulted. Anal. Calcd for $\{(NH_4)_2Ti(C_{10}O_2H_{13})_2(C_{10}O_2H_{14})\}_2 \cdot 2\ H_2O$: (fw 594.9 × 2) Ti 8.12 (8.05), C 59.02 (60.51), H 8.04 (7.56), N 2.35 (2.35). Its electronic absorption spectrum, reported here, has not been described previously. For L = DA, elemental analysis reveals one chlorine per Ti, indicating that all three dopamine groups are protonated in the solid: Anal. Calcd for $Ti(C_6H_3O_2(CH_2)_2NH_3)_3Cl \cdot 2\ H_2O$ (fw 574.9): Ti 8.72 (8.33), C 48.93 (50.1), H 6.06 (5.91), N 7.14 (7.31), Cl 5.6 (6.09).

Electrochemistry. Cyclic (scan rates of 100 mV s^{-1}) and differential-pulse voltammograms (20 mV s^{-1}) were obtained using a BAS100 electrochemical system. Glassy carbon, Pt, and SCE were used as working, counter, and reference electrodes, respectively, in a conventional H-type cell. The solutions were pH 9 (0.01 M borate buffer) with 1.0 M KCl solution at 22 ± 2 °C.

Mass Spectrometry. Solutions <0.1 mM in Ti complex were prepared in water, 1 mM HCl, or 1 mM borate buffer at pH 9 and filtered (Anotop 10, 0.2 μ) prior to injection into the ESI-MS LCQ thermopile with a capillary (T = 250 °C) voltage of 33 V, spray voltage 4.0 kV, and sheath and auxiliary gas at 40 and 26, respectively.

UV–vis spectra were measured on a Hewlett-Packard 8452A diode array spectrophotometer.

Nanoparticle Preparation and Characterization. The procedure used was adapted from that given by Gao et al.[26] for "colloid A" ($2R$ = 1 nm; R is radius) and "colloid B" ($2R$ = 4.7 nm), and particle sizes were confirmed by transmission electron spectroscopy. Titanium tetrachoride (Aldrich, 10 mL) contained in a syringe was added to 280 mL 0.1 M HCl (0.32 M final, stirred, and stored in an ice bath) at a rate of 0.5 mL/min with use of a syringe pump. Following the addition (20 min), the solution was stirred an additional 30 min, then transferred to dialysis tubing (64-mm diameter, Spectra/Por MWCO: 6–8,000), and dialyzed against 15 L of 3 mM HCl to dialysate pH 2.6. The dialysate was divided, and part A was stored in a refrigerator (4 °C) while part B was heated at 50 °C for 3 (B1) and 4 days (B2; final pH B, 2.13).

The titanium content of the nanoparticles was determined spectrophotometrically as the peroxytitanium complex[27] following hydrolysis of the nanoparticle. For the smaller particles, hydrolysis in H_2SO_4 (50 μL stock in 3 mL 3 M H_2SO_4) for 30 min at 80 °C was sufficient, while for the larger particles (B), 20 h at 95 °C was needed. The hydrolyzed solution was cooled to room temperature, 1 mL 3% H_2O_2 was added, and the sample was diluted to 10 mL. The [Ti(IV)] was determined from the absorbance at 405 nm ($\varepsilon_{Ti(IV)}$ = 750 M^{-1} cm^{-1}). For the preparation used in most of the experiments reported here, solution A was 0.25 M Ti and solution B was 0.22 M.

Results

Properties of the Titanium Complexes. Electronic absorption spectra of the complexes prepared here are

(20) Meyer, G. J. *Inorg. Chem.* **2005**, *44*, 6852–6862.
(21) Anderson, N. A.; Lian, T. *Annu. Rev. Phys. Chem.* **2005**, *56*, 491–519.
(22) Gundlach, L.; Ernstorfer, R.; Willig, F. *Physical Review B* **2006**, 74.
(23) Walters, K. A.; Gaal, D. A.; Hupp, J. T. *J. Phys. Chem. B* **2002**, *106*, 5139–5142.
(24) Harris, J. A.; Trotter, K.; Brunschwig, B. S. *J. Phys. Chem. B* **2007**, *111*, 6695–6702.
(25) Creutz, C.; Brunschwig, B. S.; Sutin, N. *J. Phys. Chem B* **2005**, *109*, 10251–10260.
(26) Gao, R.; Safrany, A.; Rabani, J. *Radiat. Phys. Chem.* **2002**, *65*, 599–609.
(27) Thompson, R. C. *Inorg. Chem.* **1984**, *23*, 1794–1798.

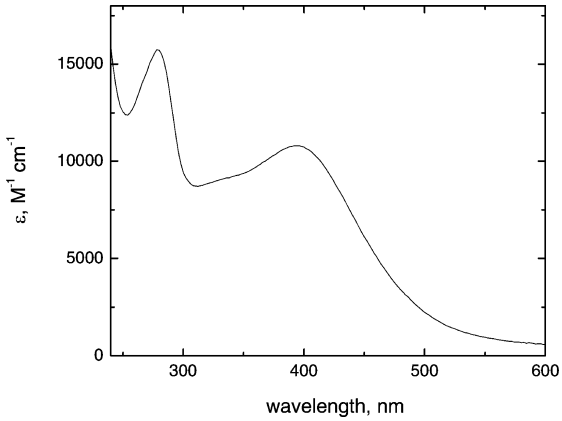

Figure 1. Electronic absorption spectrum of $(NH_4)_2[Ti(MeCat)_3]$ in ethanol.

presented in Figure 1 and in the Supporting Information Figure S1, and their features are summarized in Table 3.

For $Ti(Cat)_3^{2-}$, $(E_{pc} + E_{pa})/2$ was found to be −1.32 V versus SCE (−1.08 V vs hydrogen), in fair agreement with the value −1.38 reported previously,[8] and no anodic process was found up to +1 V. The other compounds were far less water-soluble than the catechol complex and could be characterized only by differential pulse voltammetry. The potentials obtained were all very similar, about −1.1 V versus hydrogen and close to that of the catechol complex itself, −1.08 V.

The catechol complexes were studied by electrospray ionization mass spectrometry (ESI-MS). For the catechol complex, itself, the parent anions are $[Ti(Cat)_3Na]^-$ (*m*/*z* 395) detectable only at reduced collision energy. The dopamine complex was found to both fragment and cluster, as is illustrated in the Supporting Information Figure S8 for water. Thus, the parent peak at 504 is only 30% relative intensity; the fragmentation products DAH^+ and $Ti(DAH)_2^+$ are observed at *m*/*z* 154 and 352, while cluster formation is evident above *m*/*z* > 504. When the sample was run in 1 mM HCl, only DAH^+ was observed, consistent with the expected hydrolysis of $Ti(DAH)_3^+$ in acid. With 1 mM pH 9 borate buffer, the major peaks are *m*/*z* 178 (cation, $Ti(DAH)_2H_4^{2+}$), 504 (cation, $Ti(DAH)_3^+$), 526 (cation, $Ti(DAH)_3Na-H^+$), and 524 (anion, $[Ti(DA)_3Na]^-$, as shown in Supporting Information Figure S8b,c.

Nanoparticle Characterization. Acid–Base Titration.[28] The number of positively charged ("acidic") sites on the surfaces of the nanoparticles was determined by titration with sodium hydroxide.[29] A 1.5 mL aliquot of A and stock B diluted to 10 mL was titrated by very slow addition (syringe pump 0.05 mL/min) and efficient stirring with 0.1 M NaOH and HCl, and the pH was monitored as a function of the volume of titrant. For A, 0.2 equiv OH^- (H^+) were required per TiO_2; for B, 0.14 equiv OH^- (H^+) were required per TiO_2.

$$TiOH_2 + 2OH^- \rightarrow TiO^{2-} + 2H_2O \qquad (2)$$

Particle Hydrolytic Stability. Gao et al. reported that stock solutions A and B were stable over at least 3 months.[26] Kormann et al. have reported acid-catalyzed dissolution of 3-nm particles in 0.1 M HCl with a first-order rate constant

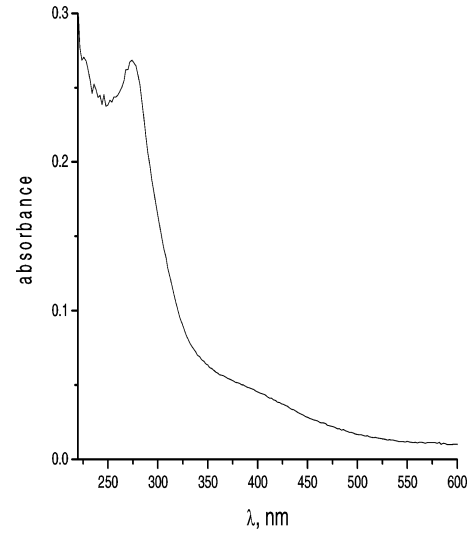

Figure 2. UV–vis spectrum of the catechol−TiO_2 (5-nm, 2.2 mM TiO_2) nanoparticle complex (0.2 mM catechol, 1-mm cell). The spectrum was corrected for TiO_2 absorption. From the equilibrium constant (vide infra) and concentrations, 95% of the catechol is bound to the TiO_2, leaving 91.4% of the TiO_2 free.

of about 1.1×10^{-3} s^{-1}.[30] The hydrolytic stability of the A particles was examined at room temperature for solutions diluted 1 to 500 in 0.1 M HCl (ca. 5% absorbance decay at 280 nm over 1 h), 3 mM HCl (<0.5% absorbance decay at 280 nm over 2 h), and water (<0.5% absorbance decay at 280 nm over 2 h). Preliminary data for the hydrolysis of particles B diluted 1 to 500 in 3 M H_2SO_4 at 95 °C are shown in the Supporting Information Figure S2; the first half-life is about 1 h.

Characterization of Catechol Binding to the Nanoparticles. To determine the UV spectrum of the nanoparticle−catechol complex we used 4.7-nm TiO_2 nanoparticle (2.2 mM) and 0.2 mM catechol in a 1-mm cell and subtracted the spectrum of the excess TiO_2. The spectrum, shown in Figure 2, resembles that in Figure 1 and the previously published spectrum of $Ti(Cat)_3^{2-}$. Note especially the intense ligand-centered band at 278 nm, which lies at 270 nm in the mononuclear complex.[8] The similarity of Figure 2 to the spectrum of $Ti(Cat)_3^{2-}$ was so great that we filtered the solution through an Amicon molecular weight 1000 membrane to remove mononuclear species and determined (from the resulting) spectrum of the filtrate that the Figure 2 is indeed the spectrum of the nanoparticle complex.

In the remaining work, the surface catechol complexes were studied in 1-cm cells in solutions obtained by diluting 0.1 mL stock A or B to 5 mL with stock catechol and water yielding solutions 5 and 4.4 mM in total Ti(IV) and (0.2–1) mM in catechol (at higher concentrations, some of the catechols gelled). The absorption spectrum of the nanoparticle complex of methylcatechol is shown in Figure 3 and Figure 4. The absorption spectra of nanoparticle complexes

(28) Stumm, W.; Logan, J. J. *Aquatic Chemistry*, Third ed.; Wiley: New York, 1996; pp 533–549.
(29) Stumm, W.; Logan, J. J. *Aquatic Chemistry*, Third ed.; Wiley: New York, 1996; pp 534–546.
(30) Kormann, C.; Bahnemann, D. W.; Hoffmann, M. R. *J. Phys. Chem.* **1988**, *92*, 5196–5201.

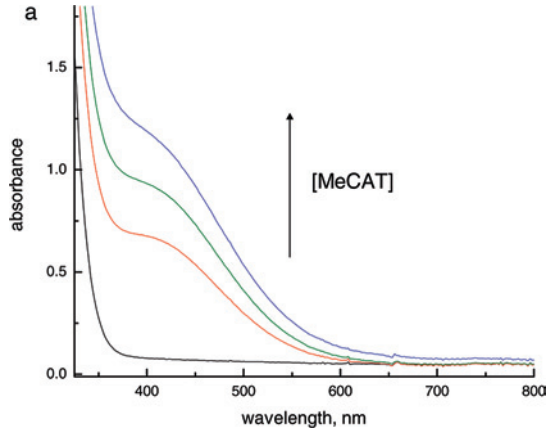

Figure 3. Absorption spectra of methylcatechol-nanoparticles for 1-nm particles and (black to red) zero, 0.2 mM, 0.4 mM, and 1 mM methyl catechol.

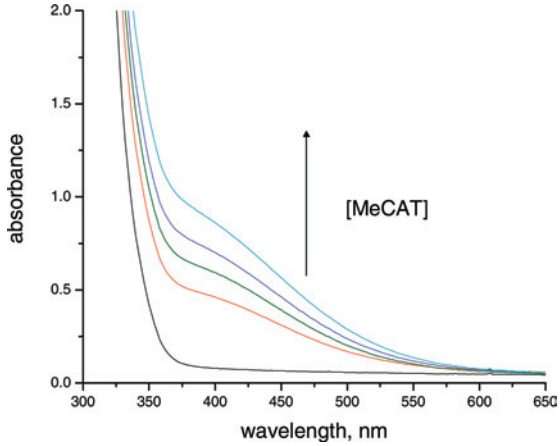

Figure 4. Absorption spectra of methylcatechol-nanoparticle for 4.7-nm (b) particles and (black to cyan) zero, 0.1 mM, 0.2 mM, 0.4 mM, and 1 mM methyl catechol at pH 3.55 ± 0.05.

of the other catechol derivatives are presented in the Supporting Information Figures S3, S4, S6, S7, S10, and S11.

We define K'_L as the equilibrium constant for binding to the nanoparticle surface at pH 3.5 (eqs 3a and 3b).

$$K'_L = \frac{[\text{NP-Ti}^{IV}\text{L}]}{[\text{LH}_2][\text{NP-Ti}^{IV}]} \tag{3a}$$

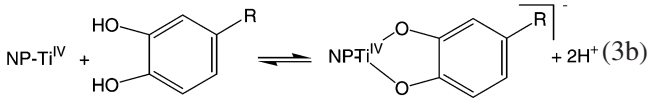

(3b)

When the absorbance data above are plotted as $1/\Delta\text{Abs}$ versus $1/[\text{H}_2\text{L}]$, $y = A + Bx$, where A is the y-intercept, B is the slope, ΔAbs is the change in absorbance at the monitored wavelength, and $[\text{LH}_2]$ is the ligand concentration, K'_L is obtained from the intercept/slope ratio (Benesi−Hildebrand analysis).[31] A Benesi−Hildebrand plot is shown for methylcatechol in Figure 5. Spectra and plots for the other catechol derivatives are given in the Supporting Information

(31) Benesi, H. A.; Hildebrand, J. H. *J. Am. Chem. Soc.* **1949**, *71*, 2703–2707.

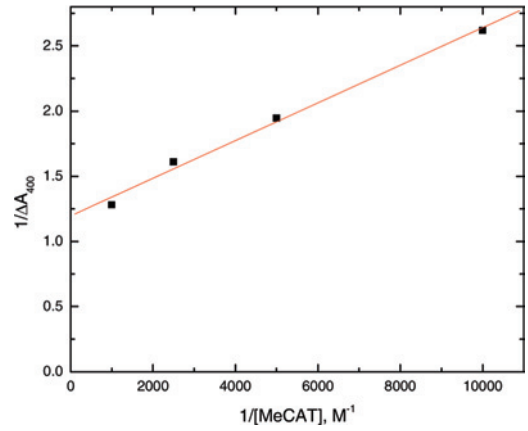

Figure 5. Benesi−Hildebrand plot for the 400-nm absorption of methylcatechol-nanoparticle spectra for 4.7-nm particles; slope $B = 1.45 \times 10^{-4}$ M^{-1}, intercept $A = 1.20$, derived $K'_L = 8.3 \times 10^3$ M^{-1}.

Table 1. Results of Benesi−Hildebrand (B−H) and Free $[LH_2]$ Analyses for TiO_2 Nanoparticles ($f_{OH}/2 = 0.1$) at 22 ± 2 °C

parameter/L	Cat	DA	MeCat	t-BuCat
		1-nm Particles		
K'_L (B−H)[a]	4×10^3	2×10^3	3.6×10^3	3.0×10^3
K'_L[b]	4×10^3	5×10^3	7×10^3	2×10^4
		4.7-nm Particles		
K'_L (B−H)[a]	1×10^4	4×10^3	8×10^3	8×10^3
K'_L[b]	4×10^3	5×10^3	7×10^3	2×10^4

[a] From Benesi−Hildebrand analyses of the $[LH_2]$ dependence of the absorbance at 374 or 400 nm, with 5 or 4.4 mM TiO_2 from solution A or B. [b] From determination of the free $[LH_2]$ following ultrafiltration.

Figures S5, S6, and S12. For the case $[\text{NP-Ti}^{IV}] \gg [\text{NP-Ti}^{IV}\text{L}]$ (eq 4),

$$\frac{[\text{TiO}_2]l}{\Delta\text{Abs}_{\text{TiL}}} = \frac{1}{K'_L \Delta\varepsilon_{\text{TiL}}[\text{LH}_2]} + \frac{1}{\Delta\varepsilon_{\text{TiL}}} \tag{4}$$

the plots of $(\Delta\text{Abs}_{\text{TiL}})^{-1}$ vs $[\text{LH}_2]^{-1}$ have y-intercept $A = (\Delta\varepsilon_{\text{TiL}}l[\text{TiO}_2])^{-1}$ and slope $B = (K'_L\,\Delta\varepsilon_{\text{TiL}})^{-1}$ where $[\text{TiO}_2]$ is the total TiO_2 concentration and $\Delta\varepsilon_{\text{TiL}}$ is the change in the molar absorptivity.

The binding constants inferred from the catechol concentration dependences are given in Table 1 and details are given in the Supporting Information Table S1.

In addition, we carried out a series of experiments with 0.1 and 0.2 mM LH_2 and 5 mM (A) or 4.4 mM (B) TiO_2 in which the free catechol concentration was determined from the 280-nm absorbance of the solution following ultrafiltration through an Amicon molecular weight 1000 membrane. These data are collected in the Supporting Information Table S3. The binding constant was then calculated from eq 2. The values so obtained are listed in the third and fifth rows of the table.

For most ligands, the K'_L values are rather similar for the 1- and 4.7-nm particles, although those for the larger particles seem about twice as large as for the smaller particles. The values also seem to vary little with the nature of the catechol. In general, values determined by the Benesi−Hildebrand method are smaller than those based on free LH_2 determination, and Rajh et al.[13] have proposed that the values inferred from the Benesi−Hildebrand method must be regarded as lower limits. However, the binding-constant

Table 2. Comparison of Binding Constants For TiO_2 and Catechols

sample	2R, nm	K'_L, M^{-1}	ref
	Catechol		
De-Gussa P-25	25	8×10^{4a}	6
DeGussa P-25	25	8.2×10^{3a}	10
De-Gussa P-25	25	4.6×10^{4b}	32
pH 6.5	400	2×10^{3c}	11
solution A	1	4×10^{3d}	*e*
solution B	4.7	1×10^{4d}	*e*
	Dopamine		
pH 3.5	4.5	7.9×10^{3d}	13
solution A	1	2×10^{3d}	*e*
solution B	4.7	4×10^{3d}	*e*
	4-Chlorocatechol		
De-Gussa P-25		10^{5a}	1, 32
	4-Nitrocatechol		
De-Gussa P-25		2×10^{6a}	1, 32

[a] Spectrophotometric analysis of supernatant after removal of TiO_2. [b] In situ ATR FTIR. [c] In situ single harmonic generation. [d] From Benesi–Hildebrand plot. [e] This study.

values determined from the free LH_2 concentration following removal of the TiO_2 could be artificially high if the catechol decomposes to some extent during the separation process.

Discussion

Following Gao, we prepared "1-" and "4.7"-nm nanoparticles. On the basis of the density of TiO_2 anatase, 3.9, these correspond approximately to the compositions $(TiO_2)_n$ with n of the order of 20 and 2000 for the small and larger nanoparticles, respectively. For the latter about one-third of the Ti atoms are on the surface. From the acid–base titration, the concentrations of binding sites are 0.5 mM and 0.3 mM for the diluted solutions used.

Complexation. It is of interest to compare the binding for the various particles and to try to determine to what extent the binding sites differ among the different materials. Moser at al.[6] characterized the Langmuir adsorption on 0.5 g/L 10-nm TiO_2 (6×10^{-3} M TiO_2, 2×10^{-4} M particles) with adsorbate concentrations in the range from 0.1×10^{-4} to 4×10^{-4} M to obtain $K = 8 \times 10^4$ M^{-1} for catechol itself. Rodriguez et al.[10] characterized the binding of catechol to anatase P-25 in terms of Langmuirian constants $K_L = 8.2 \times 10^3$ M^{-1} and $\Gamma_{max} = 1.25 \times 10^{-6}$ mol m^{-2} and found the adsorption isotherms to be independent of pH in the range 3.65–6.0. Rajh et al.[13] considered the binding of dopamine to 4.5-nm TiO_2 colloids containing 1.7×10^{-4} M particles, with 405 surface titanium sites. Two distinct dopamine concentration ranges were observed: for <0.5 mM dopamine, $K = 7.9 \times 10^3$ M^{-1}; at higher dopamine, $K = 54$ M^{-1}. Catechol binding to TiO_2 has been studied by in situ single harmonic generation, and Langmuirian data treatments yielded 2×10^3 M^{-1}.[11] The results of the literature studies of TiO_2 binding to selected catechol derivatives are summarized in Table 2 in which they are compared with the present results.

The binding constants to TiO_2 nanoparticles are not very sensitive to the nature of the catechol; nor evidently do they depend greatly on particle size. For the dependence of binding on the nature of the catechol, it is said that the affinity of the surface for the doubly deprotonated ligands parallels the Brönsted acidity of the surface.[32] Interestingly, Lian has found that rates of back electron transfer *do* depend on the nature of the catechol.[7]

Table 3. Electronic Absorption Spectra and Electrochemical Data for the Ti(IV) Complexes

complex	λ_{max}, nm (log ε_{max}, M^{-1} cm^{-1})	$E_{1/2}$-, V vs NHE[d]
$(NH_4)_2\{Ti(Cat)_3\}$	369 (3.97), 340 sh, 270 (4.32)[a]	−1.03
1-nm NP-Ti(Cat)	$\varepsilon_{374} = 3.1 \times 10^3$	[−1.08[e]]
4.7-nm NP-Ti(Cat)	$\varepsilon_{374} = 2.6 \times 10^3$	
$Ti(DAH)_3Cl$	388 (4.04), 333(sh), 275 (4.32)	−1.00
1-nm NP-Ti(DAH)	$\varepsilon_{400} = 2.2 \times 10^3$	
4.7-nm NP-Ti(DAH)	$\varepsilon_{400} = 1.2 \times 10^3$	
$(NH_4)_2\{Ti(MeCat)_3$	394 (4.04), 335(sh), 278 (4.20)[b]	−0.99
4.7-nm NP-Ti(MeCat)	$\varepsilon_{400} = 2.6 \times 10^3$	
$(NH_4)_2\{Ti(tBuCat)_2(HtBuCat)\}_2$	330 (3.67), 276 (4.04)[b,c]	−1.03

[a] From reference 8. [b] Iin ethanol. [c] Molar absorptivity per Ti. [d] Obtained from the cathodic peak from a differential pulse voltammogram (corrected for half-the peak width) measured with a pyrolytic graphite electrode (20 mV/s) for a pH 9 (0.01 M borate buffer), 1.0 M KCl solution at 22 ± 2 °C. [e] $(E_{pc} + E_{pa})/2$ from cyclic voltammetry.

Ti(IV) has an extremely high affinity for ligands of the catechol type, with which it forms strong chelates. For the mononuclear species in eq 1, $\log(\beta_3)$ for formation of the tris-chelate of catechol[8] is 60, and the average value per binding step $\log(\beta_{av})$ is 20. This parameter is analogous to K_{TiL} (elsewhere denoted $K_L{}^{2-}$)[32] for eq 5, which is obtained

(5)

by correcting for the ionization constants of catechol.[8] A value $\log(K_{TiL}) \sim 26$ thereby results, indicating very tight binding of catechol to the nanoparticles, to which the catechol is also chelated.[13]

Spectroscopy. The electronic absorption spectra of the TiL_3 complexes for L = Cat, dopamine, and MeCat are very similar (Table 3, Supporting Information Figures S2−S4), with LMCT absorption maxima at 375–390 nm and ε_{max} of about 1.0×10^4 $M^{-1}cm^{-1}$. The complex formed with t-butyl catechol has a different structure. The coordination shell about each titanium in the bridged species formula contains only two chelated dianions, and one of the bidentate anions is shared by the two titanium ions. In addition, the coordination shells are rather distorted when compared to that of the tris(catecholate) complex.[8] Thus, the electronic absorption spectrum would be expected to differ from those of the tris complexes, although is worth noting that the major difference, apart from the shift of the LMCT maximum to ~330 nm, is in the reduced intensity of ($\varepsilon_{Ti,330} = 4.37 \times 10^3$ M^{-1} cm^{-1}) the LMCT transition which might be expected from the reduced number of L^{2-} chelated to Ti^{IV}.

The absorption spectra of TiL_3 complexes and L-bound TiO_2nanoparticles are compared in Table 3. The TiL_3 and

(32) Araujo, P. Z.; Morando, P. J.; Blesa, M. A. *Langmuir* **2005**, *21*, 3470–3474.

L-nanoparticle complexes exhibit a ligand-centered band near 280 nm and an asymmetric LMCT band to longer wavelength (Figures 1 and 2). Catechol (LH_2) is oxidized at +1.06, and doubly deprotonated catechol (L^{2-}) is oxidized at +0.043 V versus hydrogen.[33] Taking the protonated ligand as a model for that bound to Ti(IV) and using the potential given in Table 3, the LMCT in the mononuclear complex should lie at $\Delta E^0 + \lambda$ (the reorganization energy). Estimating ΔE^0 as $1.06 - (-1.08) = 2.14$ eV implicates a λ value of 1.2 eV. In principle, the Ti(IV) center in the nanoparticle is a better oxidant than in the tris catecholate complexes. Grätzel has given $E_f = +0.13 - 0.059$ pH[34] (−0.2 V at pH 3.5), and Dimitrijevic et al. found dopamine-capping to reduce the potential an additional 0.1 V.[35]

Then the ΔE^0 for LMCT in a nanoparticle−catechol complex to an acceptor state at the bottom of the conduction band is $1.06 - (-0.2) = 1.26$ eV (983 nm). If λ is the same as for the tris complex (1.4 eV), the 392-nm (3.16 eV) peak would involve an acceptor level ~0.5 eV above the bottom of the conduction band. A similar acceptor level has been proposed by Harris et al.[24] The maxima of the LMCT bands do shift to lower energy as the catechol is substituted with electron-donating groups, as expected for LMCT; thus, the order dopamine ~ methylcatechol > catechol.

The asymmetry of the lowest energy TiL_3 band is apparently due to a shoulder near 330 nm. We suggest that the two bands arise because Ti πd acceptor orbitals are split by the ligand field, which is of lower symmetry than octahedral in the tris complex. This assignment is consistent with electronic structure calculations.[36,37]

It is also of interest to compare the intensities of the LMCT transitions in the mononuclear and nanoparticle complexes. To obtain molar absorptivity values for the latter, we assume that the number of active sites for catechol bonding is identical to $\alpha/2$ (determined in eq 1). The molar absorptivities at 400 nm then all lie in the range $(2–3) \times 10^3$ M^{-1} cm^{-1}, typically about one-third that of the mononuclear tris complex, consistent with a localized LMCT assignment for nanoparticle complexes.

Rajh et al. have noted the colors of catechol-type adsorbates (e.g, see Figure 1 in ref 13).[16,38,39] Figure 6 provides an explanation for the observed colors of the nanoparticles[13] and the mononuclear complexes. As was already noted in 1984 for $Ti(Cat)_3^{2-}$, the colors of both complexes and nanoparticles arise simply because the intense UV LMCT absorption tails far into the visible region in both cases.

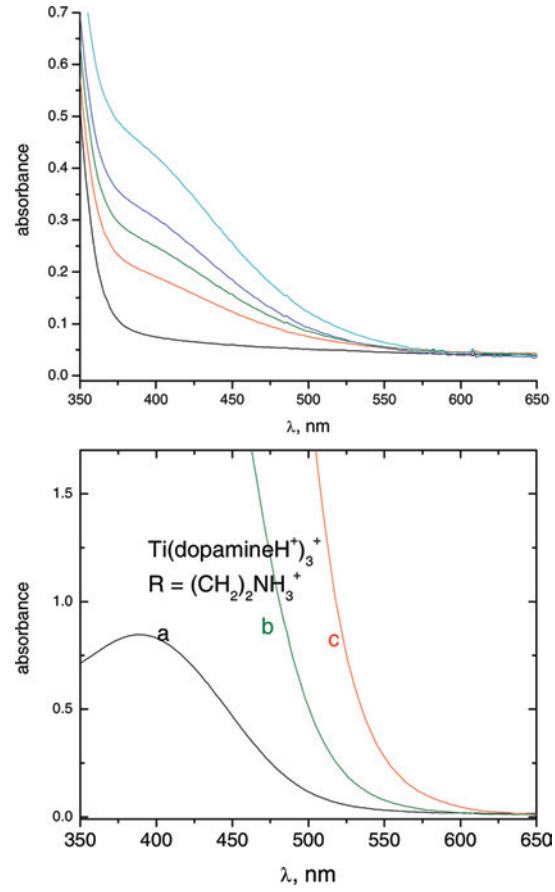

Figure 6. (top) Spectra of dopamine-bound 5-nm TiO_2 nanoparticles with 0.0, 0.1, 0.2, 0.3, and 0.4 mM dopamine and (bottom) of the tris-dopamine complex in water: (a) 6.5. $\times 10^{-4}$ M, 0.2 cm cell, (b) 1 cm cell, and (c) saturated solution.

Concluding Remarks

The $Ti^{IV}L_3$ reduction potentials are not very sensitive to the nature of the catechol; nor evidently are the binding constants to TiO_2 nanoparticles. The binding constants for TiO_2 nanoparticles do not depend greatly on particle size. The nanoparticle colors are attributed (as are the colors of the TiL_3 complexes) to the tails of the about 400-nm LMCT bands.

Acknowledgment. This research was carried out at Brookhaven National Laboratory under contract DE-AC02-98CH10886 with the U.S. Department of Energy, supported by its Division of Chemical Sciences, Geosciences, and Energy Biosciences, Office of Basic Energy Sciences. We thank E. Sutter and S. Lymar for the TEM measurements and B. Brunschwig, T. Lian, and T. Rajh for sharing their unpublished results with us.

Supporting Information Available: Spectra of L and Mononuclear Titanium(IV) $Ti^{IV}L_3$ Complexes; TiO_2-L Nanoparticle Spectra and Plots (PDF). This material is available free of charge via the Internet at http://pubs.acs.org.

IC701687K

(33) Steenken, S.; Neta, P. *J. Phys. Chem.* **1979**, *83*, 1134–1137.
(34) Duonghong, D.; Ramsden, J.; Grätzel, M. *J. Am. Chem. Soc.* **1982**, *104*, 2977–2985.
(35) Dimitrijevic, N. M.; Saponjic, Z. V.; Bartels, D. M.; Thurnauer, M. C.; Tiede, D. M.; Rajh, T. *J. Phys. Chem. B* **2003**, *107*, 7368–7375.
(36) Persson, P.; Bergstrom, R.; Lunell, S. *J. Phys. Chem. B* **2000**, *104*, 10348–10351.
(37) Duncan, W. R.; Prezhdo, O. V. *J. Phys. Chem. B* **2005**, *109*, 365–373.
(38) Rajh, T.; Chen, L. X.; Lukas, K.; Liu, T.; Thurnauer, M. C.; Tiede, D. M. *J. Phys. Chem. B* **2002**, *106*, 10543–10552.
(39) de la Garza, L.; Saponjic, Z. V.; Dimitrijevic, N. M.; Thurnauer, M. C.; Rajh, T. *J. Phys. Chem. B* **2006**, *110*, 680–686.